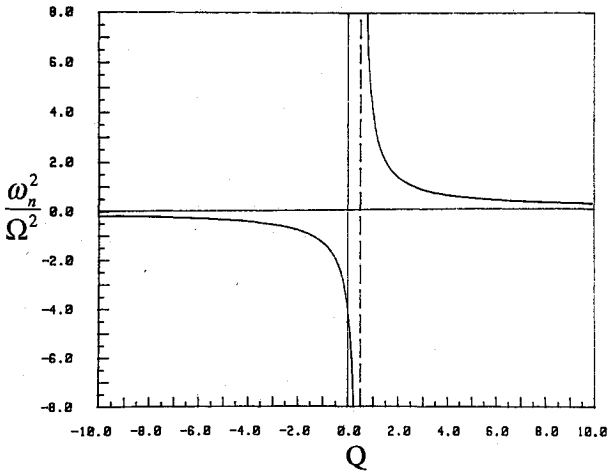

Fig. 2 Full-field Liapunov stability boundary for $b \gg c$ (i.e., thin panels for which $\beta \approx 1$).

Conditions I and II do not depend on the flexibility of the satellite. Since the moments of inertia A, B, and C of the entire undeformed satellite are defined as

$$A = A_c + 2m\ell^2 + 2C_p, \qquad B = B_c + 2B_p$$

$$C = C_c + 2m\ell^2 + 2A_p$$

we see that conditions I and II reduce to the requirement that $C > B > A$, the stability conditions for a gravity gradient stabilized rigid body discussed by DeBra and Delp.[2]

Condition III involves the flexibility of the satellite and III′ expresses this condition in terms of nondimensional parameters. Note that $\beta = (b^2 - c^2)/(b^2 + c^2)$. Therefore, since $b > c$, we have in general that $0 < \beta < 1$. Also, for most panels $b \gg c$, so $\beta \approx 1$. Assuming that $\beta = 1$, it is useful to look at a plot of the curve $(\omega_n^2/\Omega^2) = 4/(2Q - 1)$ since it gives the stability boundary of condition III′ (Fig. 2). Since $A_p - C_p > 0$, it can be shown that conditions I and II imply $Q > \frac{1}{2}$ or $Q < 0$ so the domain of Q is $(-\infty, 0) \cup (\frac{1}{2}, \infty)$. Note that for $Q < 0$, the quantity $4\beta/(2Q - 1)$ is negative in which case condition III′ is trivially satisfied.

As the plot in Fig. 2 shows, the critical parameter value is $Q = \frac{1}{2}$ since near this point the torsional stiffness becomes a significant factor. It is interesting to note that $Q = \frac{1}{2}$ when $A = C$. Since $C > B > A$, we have that $Q \approx \frac{1}{2}$ implies $A \approx B \approx C$. Thus, the region for which $Q \approx \frac{1}{2}$ is near the origin of the k_1—k_2 DeBra-Delp graph.[2] Recall that the gravity gradient torque goes to zero at the origin of this graph. What these results indicate is that the torsional stiffness plays an increasingly significant role as the magnitude of the gravity gradient torque vector approaches zero.

The fact that condition III′ is easily satisfied as long as Q is not close to $\frac{1}{2}$, along with the fact that condition III′ is automatically satisfied for all values of torsional stiffness if $Q < 0$, suggests that the use of guy wires to restrict vibrations to purely torsional modes can significantly improve attitude stability.

Acknowledgment

The authors wish to thank Professor Willy Hereman (Mathematics Department, University of Wisconsin at Madison) for writing the MACSYMA code used to calculate the Hessian matrix and evaluate its determinants.

References

[1]Meirovitch, L., *Methods of Analytical Dynamics*, McGraw-Hill, New York, 1970.

[2]DeBra, D. B., and Delp, R. H., "Rigid Body Attitude Stability and Natural Frequencies in a Circular Orbit," *Journal of the Astronautical Sciences*, Vol. 8, 1961, pp. 14–17.

Results in Identification of a Flexible Structure Using Lattice Filters

M. D. Roesler*
TRW Space and Defense Group, Redondo Beach, California 90278
and
F. Jabbari†
University of California at Irvine, Irvine, California 92717

Introduction

THE main challenge in applying adaptive identification and control techniques to flexible structures arises from model order selection. Since the effective order of such systems varies with the number of substantially excited modes, the order of the algorithm cannot be fixed a priori. In the case of large space structures, maneuvers such as docking or on-orbit assembly may excite different sets of structural modes causing the system to be time varying as well as order varying. Knowledge of the system order (or maximum order) is typically needed for most identification and control methods. The lattice filter, recursive in time and order, does not require the model's order to be fixed a priori. This order-recursive property can be used to identify the system order on-line and to update the order of the parameter estimator for identification or control purposes.

The vector-channel lattice filters used here are based on the derivation in Ref. 1, where simulation results were presented for a hub-flexible beam. Also, in Ref. 2, vector-channel lattice filters were used to identify the natural frequencies of the NASA-Langley grid structure. The system in Ref. 2 was a high-order single-input/single-output (SISO) system with only slight variations in parameters (see Ref. 2 for further details). A somewhat similar approach was taken in Refs. 5 and 6 for the identification of flexible systems where order-recursive methods were used to obtain some of the results. Here, the lattice filter is solely used to identify an experimental truss structure (Fig. 1), which is a flexible multi-input/multi-output (MIMO) system. Previous experimentation on the truss[3] has shown its fundamental mode of vibration at 0.68 Hz and its 20th mode at 45 Hz. Preliminary results with comparisons to other identification methods were presented in Ref. 4. Here, the on-line identification of the structure's low-frequency dynamics using vector-channel lattice filters is considered for two important cases: 1) time-varying, in which the system undergoes a sudden variation in characteristics with a corresponding change in effective order; and 2) multi-input, in which the structure is excited simultaneously with all of its actuators (a total of four inputs). The vector-channel lattice filter is shown to perform well in both of these instances.

Problem Statement

The damped structural system's forced response is modeled by a finite-order differential equation of the following form:

$$M\ddot{x} + D\dot{x} + Kx = Bu \tag{1}$$

where x is the $n \times 1$ generalized displacement vector, and u is

Received Sept. 6, 1989; revision received Feb. 14, 1990. Copyright © 1990 by the American Institute of Aeronautics and Astronautics, Inc. All rights reserved.

*Member, Technical Staff, Control Systems Engineering Department, One Space Park, R9/2139.

†Assistant Professor, Department of Mechanical Engineering. Member AIAA.

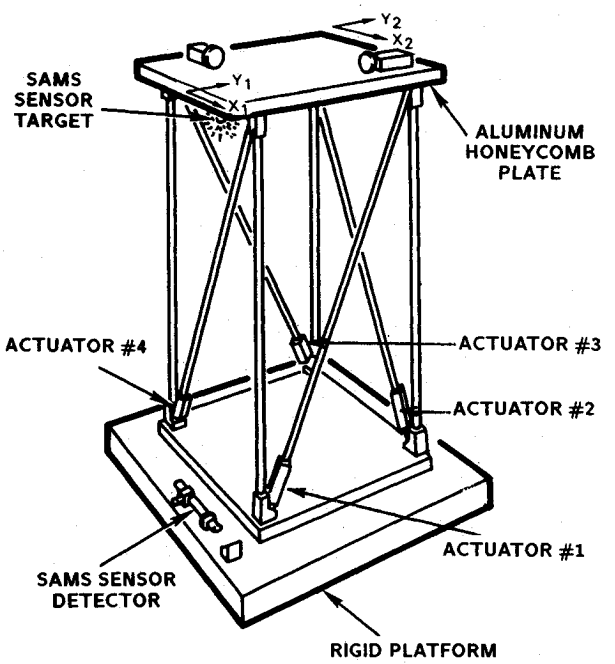

Fig. 1 Truss structure.

the $m \times 1$ input vector. M, D, and K are the symmetric $n \times n$ mass, damping, and stiffness matrices, respectively. B is the $n \times m$ input matrix. Finally, n is the number of substantially excited modes. In the identification literature, it is common to consider the following input-output autoregressive moving average (ARMA) representation of the discretized version of Eq. (1):

$$y(t) = \sum_{i=1}^{2n} a_i y(t-i) + \sum_{j=1}^{2n} b_j u(t-j) \tag{2}$$

where $y(t)$ is the $p \times 1$ measurement vector. The a_i are the AR coefficients and the b_j are the MA coefficients. The a_i and b_j are generally matrices for MIMO systems and reduce to scalars for SISO systems. The model in Eq. (2) can be put in any of the canonical forms if needed. In particular, for controllable and observable SISO systems, the order of the ARMA model is the same as the order of the state space representation, and the a_i yield the characteristic polynomial of the system. If there are more than one input or output, the a_i are matrices, and the preceding interpretation is not necessarily valid. Typically, the order of the ARMA is less than $2n$. For this case, Wiberg[7] suggested an alternative where all sensors are forced to observe the same system dynamics by constraining the a_i in Eq. (2) to be exactly $2n$ scalars, i.e., the negatives of the coefficients of the characteristic polynomial. This representation is useful for order determination and can be extended to the case of several sets of sensors by forcing each sensor within a set to see common dynamics. The vector-channel lattice filter derived in Ref. 1 incorporates this representation. In the experiment considered here, the sensors are constrained to see the same system dynamics, such that the a_i of Eq. (2) are scalars, and the b_j are $p \times m$ matrices. Once Eq. (2) is identified, the system poles are found by extracting the roots of the characteristic polynomial.

The order recursiveness of the lattice filter is an attractive feature for the identification of flexible structures because the order of these systems may vary with time. A lattice filter algorithm of order N, recursive both in time and order, yields filters of order one to N automatically. The algorithm also allows the maximum order of the filter to be increased gradually without reprocessing previous data. Since all intermediate filters are automatically obtained, the effective order of the system can be identified and the estimator determined accordingly. Another interesting property of the lattice algorithm is its applicability in parallel processing. Only the main lattice algorithm (forward and backward residual errors) need be executed at each time step. Algorithms for determining the ARMA coefficients, the natural frequencies, and/or the one-step-ahead prediction can be executed at separate times on different processors.

Table 1 Autoregressive moving average coefficient algorithm

For $n = 1, N; j = 1,n$

$$\gamma_{n+1,j}(t) = \gamma_{n,j}(t) - \beta_{n,j}(t) R_n^{-r}(t) \bar{r}_n^T(t) \gamma_n(t)$$

$$\beta_{n+1,j+1}(t) = [\beta_{n,j}(t) - \gamma_{n,j}(t) \bar{r}_n(t)] - \alpha_{n,j}(t) R_n^{-e}(t) K_{n+1}(t)$$

$$\alpha_{n+1,j}(t) = \alpha_{n,j}(t) - [\beta_{n,j}(t) - \gamma_{n,j}(t) \bar{r}_n(t)] R_n^{-r}(t-1) K_{n+1}^T(t)$$

End conditions: for $n = 0, 1 \ldots, N-1$

$$\alpha_{n+1,n+1}(t) = R_n^{-r}(t-1) K_{n+1}^T(t)$$

$$\beta_{n+1,1}(t) = R_n^{-e}(t) K_{n+1}(t)$$

$$\gamma_{n+1,n+1}(t) = R_n^{-r} \bar{r}_n^T(t) G_n(t)$$

To illustrate these properties, the ARMA coefficient algorithm is given in Table 1. This is the same algorithm as presented in Ref. 2, page 550, Table 2, except that the A, B, and C, are replaced with α, β, and γ to avoid confusion with Eqs. (1) and (2). The main lattice prediction algorithm is given in Ref. 2, page 549, Table 1. The different quantities appearing in the algorithm are fully described in Ref. 2 as well. The $\alpha_{n,j}$ coefficients in the ARMA algorithm contain both the a_i and the b_j of Eq. (2) for an nth-order filter. The dimensions of α, β, and γ depend upon the number of channels in the lattice filter. The channels are determined by the number of inputs, outputs, and type of embedding.[2] For instance, in the case of a SISO filter, the α, β, and γ are 2×2 matrices, the estimate of the AR coefficient a_i is the (1,1) element of $\alpha_{n,i}$, and the estimate of the MA coefficient b_i is the (1,2) element of $\alpha_{n,i}$.

Experimental Results

Experimental Setup

The experimental truss structure is shown in Fig. 1. The top and bottom aluminum honeycomb plates are assumed to be rigid bodies whose relative position must be controlled with high accuracy. The bottom plate is clamped securely to the ground. Separating the plates is a flexible aluminum truss structure consisting of four load-bearing corner posts and four diagonal members, which are nominally not loaded but contain linear magnetic actuators for active structural control. The posts lie at the corners of a square 55 in. on a side; the plate-to-plate distance is approximately 115 in. The surface accuracy measurement system (SAMS) sensors yield four measurements X_1, Y_1, X_2, and Y_2, which are the relative displacements of the top plate with respect to the bottom plate at the two diagonally opposite corners shown in Fig. 1. The sensors operate at a maximum rate of 200 Hz, and each 16-bit sensor word interfaces directly to the processor. The voice coil type actuators have a throw range of approximately ± 0.10 in. and produce a maximum force of 11 lb. The computer system consists of an NMX-432 Numerix Array Processor hosted by a DEC μVAX II minicomputer. An eighth-order 5-channel (2-input 2-output) lattice prediction algorithm can operate at sample rates up to 100 Hz and a 16th-order filter up to 52 Hz.

Previous testing[3] has shown that the structure has three modes below 1 Hz. There are two lateral modes at 0.68 Hz: one along X and the other along Y. The third mode is the rotation of the top plate about the vertical Z axis, and its natural frequency is around 1 Hz. In the following, the structure's modal frequencies ω and modal damping ratios ζ are determined by extracting the complex conjugate discrete

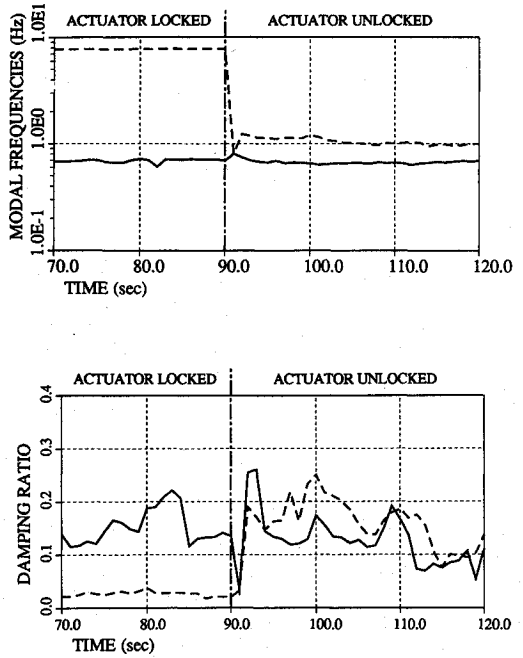

Fig. 2 Modal frequencies and damping ratios.

domain poles (z_p, $\bar{z}_p$) from the system's characteristic polynomial (determined by the AR coefficients) and by considering the following relationship, where T is the sampling period: $\ln(z_p)/T = -\zeta\omega + j\omega\sqrt{1-\zeta^2}$.

Time Varying System: Order Determination

The truss structure is rendered time varying by pinning one of the actuators during the first part of the test and releasing it during the remainder of the test. Locking the actuator increases the structure's stiffness in the direction of the actuator; unlocking it restores the original stiffness to the system. The contrast is abrupt; not only is there a change in the system's effective order, but one of the system's fundamental frequencies shifts from the neighborhood of 8-1 Hz.

The excitation sequence is [0.5 Hz, 12 Hz] bandlimited digital white noise sampled at 50 Hz. The structure is excited with the actuator labeled 1; the other three actuators are not powered. Close to 90 s of data are recorded with actuator 4 locked, then actuator 4 is released. The results presented in Fig. 2 are from a 30th-order SISO lattice filter (see the following for discussion of filter order). A forgetting factor of 0.99 is used in the lattice algorithm, so that the filter can adapt itself to the time-varying characteristics. The forgetting factor is a scalar λ ($0<\lambda\leq 1$) often introduced in order to weight past data. For $\lambda = 1$, past and present data are equally weighted (typical of time invariant applications), and for $\lambda<1$, past data are discarded exponentially (time-varying applications). See Refs. 1 or 2 for details. Figure 2 shows the system poles detected by the algorithm before and after the change. When actuator 4 is locked, the lattice finds two modes: one at 7.8 Hz with 0.025 damping and one at 0.7 Hz with approximately 0.15 damping. The 7.8-Hz mode vanishes as the actuator is unlocked. Within 2 s of the unlocking, the lattice filter determines a new mode in the neighborhood of 1 Hz: a significant change in system characteristics detected within seconds. Another 10 s are required for the lattice to converge to the true value. The chatter observed on the damping ratio curves of Fig. 2 can be explained by the forgetting factor $\lambda<1$, which renders the filter more responsive to small variations; also, damping ratio estimates are known to be more sensitive than frequency estimates.

The quantity considered for estimating the effective system order is the R_n^e matrix, which is the norm of the forward

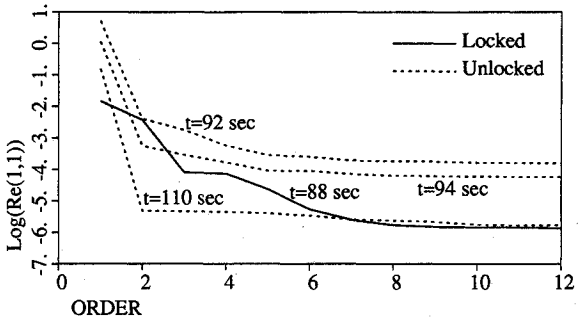

Fig. 3 Effective system order during time-varying test.

residual error in the lattice filter. The nth-order residual error is the portion of the system measurement that cannot be fit in an nth-order model based on all previously collected data. In particular, the (1, 1) element of R_n^e corresponds to the norm of the nth-order forward residual error and is the quantity used for order estimation. Most criteria for order determination rely heavily on a quantity similar or identical to R_n^e (1, 1). (See Refs. 8 and 9.) The lattice filter automatically provides this term for all orders, so that order determination algorithms can be implemented easily with the lattice algorithm. For systems exhibiting low noise and good linearity characteristics, the behavior of R_n^e (1, 1) itself is a good indicator of effective system order, as seen in this application. Figure 3 shows plots of the log [R_n^e (1, 1)] vs order n for the actuator locked and actuator unlocked cases at different times. The point at which the curve settles to a slowly decreasing slope is indicative of the effective order of the system as the higher-order terms no longer contribute significantly to the reduction of the error norm. Prior to unlocking the actuator (solid curve at $t = 88$ s), the system is fit by a sixth- to eighth-order model; however, the drop in the curve at order 4 suggests that the effective order is 4. Recall that actuator 4 is released at approximately $t = 90$ s. The dashed curves of Fig. 3 show the evolution of the system order as the transients die out and the lattice adapts to the new system characteristics. As time increases, the drop at order 2 becomes more pronounced, which indicates that only one mode is substantially excited.

Although the lattice suggests the system's effective order to be 4 with the actuator locked and 2 in the unlocked configuration, a filter with an order as large as 30 is used to determine system fundamental frequencies and damping ratios. A high-order filter is able to identify both the poorly excited modes and the substantially energized modes. System noise and nonlinearities, such as stiction in the actuators, are fit into higher-order terms allowing the system's fundamental characteristics to be observed more accurately. In time varying tests, where the forgetting factor is typically less than 1, the filter is more sensitive to small fluctuations. The high-order lattice filter tends to smooth out these curves. On the other hand, the effective system order is representative of (twice) the number of substantially excited modes only. In order to determine these modes precisely (and possibly poorly excited modes), much higher-order lattice filters are required. This has been observed previously in several applications.[2,5] Here, the lattice determines two significantly excited modes in the locked configuration. Indeed, two modes are identified, and two very distinct peaks are observed in the frequency response.[4] In the unlocked configuration, the structure is found to have only one substantially excited mode; however, two modes are determined from the ARMA algorithm. This is consistent with the frequency response where one large peak is observed at 0.68 Hz with a smaller hump close to it at 1 Hz.[4] At low orders, the lattice combines the two modes together. At higher orders, the two modes can be distinguished. For instance, a 10th-order lattice filter finds only one fundamental frequency at 0.78 Hz with 0.18 damping in the unlocked configuration, but the filter determines the two modes of the locked system. By extracting system poles for all successive orders in the lattice

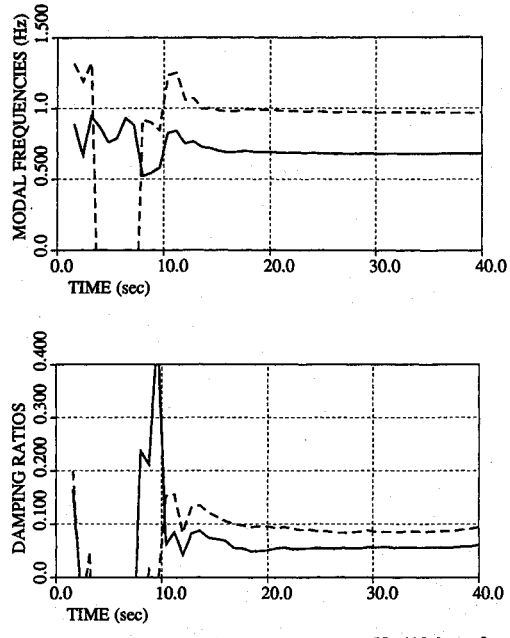

Fig. 4 System poles 4-input/1-output sensor X_1 (18th-order lattice).

algorithm, the two closely spaced modes can be progressively distinguished. Extraneous poles due to noise and/or nonlinearities are recognized by their erratic nature; whereas genuine system poles behave consistently.

Multi-Input System

For the multi-input time-invariant case, data are recorded while all four actuators are simultaneously excited. The input sequences are digital white noise bandlimited between 0.25 and 2 Hz sampled at 12.5 Hz in order to excite the low-frequency dynamics of the structure. The system poles are successively extracted for 4-input/1-output and 4-input/4-output configurations.

Sensor X_1 data are run through an 18th-order 4-input/1-output lattice filter. The resulting modal frequencies and damping ratios for sensor X_1 are shown in Fig. 4: one mode at 0.97 Hz with 0.09 damping and another mode at 0.68 Hz with 0.06 damping. Similar results, not shown, are obtained by running sensor Y_1 data through an 18th-order 4-input/1-output lattice filter: one mode at 0.97 Hz with 0.09 damping and one at 0.68 Hz with 0.09 damping. Structural analysis of the truss shows one torsional mode and two lateral modes, one along X and one along Y. Thus, sensor X_1 sees the torsional and X-lateral modes, and sensor Y_1 the torsional and Y-lateral modes. From the results, it can be deduced that the 0.97-Hz mode is the torsional mode since the damping is the same on both X_1 and Y_1, whereas the two lateral modes are at 0.68 Hz as proved by the difference in damping ratios. Previous single-input identification testing with lattice filters had not clearly revealed the existence of two modes at the same frequency. With a single actuator exciting the structure, the torsional and only one of the lateral modes are significantly excited (see Ref. 4 for results pertaining to this case). The multi-input excitation provides a richer picture of the system's dynamics.

The MIMO data are run through an 18th-order 4-input/4-output lattice. All sensors X_1, X_2, Y_1, and Y_2 are constrained to see the same dynamics. The outcome is a 0.97-Hz mode with 0.09 damping and a 0.68-Hz mode with 0.07 damping. The lattice filter has merged the two lateral modes into a single mode because it is not configured to separate X dynamics from Y dynamics. To ensure that both lateral modes are distinguished, the lattice should be set up so that X sensors (X_1, X_2) and Y sensors (Y_1, Y_2) observe different dynamics, in which case the a_i would be 2×2 matrices.

Conclusion

The vector-channel lattice filter was used to identify the truss experiment's modal frequencies and damping ratios for two important cases: a time-varying system with order change and a multi-input system configuration. The time-varying test was special in that the variation in parameters was significant as well as sudden, but, more importantly, the effective order of the system changed. The lattice filter adapted promptly to the parameter changes and was shown to detect order changes in the system. The multi-input data was found to give a better picture of system dynamics than single-input data, especially for the system damping ratios. These results suggest that the vector-channel lattice filter is an efficient on-line identification tool with applications in adaptive identification and control.

References

[1]Jabbari, F., and Gibson, J. S., "Vector Channel Lattice Filters and Identification of Flexible Structures," *IEEE Transactions on Automatic Control,* Vol. 33, No. 5, May 1988, pp. 448–456.

[2]Jabbari, F., and Gibson, J. S., "Adaptive Identification of Flexible Structures by Lattice Filters," *Journal of Guidance, Control, and Dynamics,* Vol. 12, No. 4, 1989, pp. 548–554.

[3]Lukich, M. S., "System Identification and Control of the Truss Experiment: A Retrospective," AIAA Paper 88-4152, Aug. 1988.

[4]Roesler, M. D., Jabbari, F., Lukich, M. S., and Gibson, J. S., "Identification of a Flexible Truss Structure Using Lattice Filters," *Proceedings of the American Control Conference,* Atlanta, GA, June 1988, American Automatic Control Council, Green Valley, AZ, pp. 1474–1482.

[5]Sundararajan, N., and Montgomery, R. C., "Identification of Structural Dynamics Systems Using Least-Squares Lattice Filters," *Journal of Guidance, Control, and Dynamics,* Vol. 6, No. 5, 1983, pp. 374–381.

[6]Sundararajan, N., and Montgomery, R. C., "Adaptive Modal Control of Structural Dynamics Systems Using Recursive Lattice Filters," *Journal of Guidance, Control, and Dynamics,* Vol. 8, No. 2, 1985, pp. 223–229.

[7]Wiberg, D. M., "Frequencies of Vibration Estimated by Lattices," *Journal of Astronautical Sciences,* Vol. 33, No. 1, 1985, pp. 35–47.

[8]Lee, D. T. L., "System Order Estimation of ARMA Models by Ladder Forms," *Proceedings of the American Control Conference,* American Automatic Control Council, Green Valley, AZ, 1983, pp. 1002–1007.

[9]Rissanen, J., "Modeling by Shortest Data Description," *Automatica,* Vol. 14, No. 5, 1978, pp. 465–471.

Dynamic Decrease of Drag by Optimal Periodic Control

Gottfried Sachs*
Technische Universität München, 8000 Munich 2, Germany

Introduction

RECENTLY, periodic cruise as opposed to the well-known steady-state cruise has acquired great interest since this type of an unsteady cruise offers a possibility for reducing the fuel consumption of aircraft. For a wide range of aircraft models, steady-state cruise is nonoptimal.[1] Numerical

Received Dec. 13, 1989; revision received April 7, 1990. Copyright © 1990 by the American Institute of Aeronautics and Astronautics, Inc. All rights reserved.

*Professor, Director of the Institute of Flight Mechanics and Flight Control. Associate Fellow AIAA.